THE JOURNAL OF BIOLOGICAL CHEMISTRY VOL. 287, NO. 49, pp. 41446–41457, November 30, 2012
© 2012 by The American Society for Biochemistry and Molecular Biology, Inc. Published in the U.S.A.

Studies on the Substrate and Stereo/Regioselectivity of Adipose Triglyceride Lipase, Hormone-sensitive Lipase, and Diacylglycerol-*O*-acyltransferases*

Received for publication, July 12, 2012, and in revised form, October 12, 2012 Published, JBC Papers in Press, October 12, 2012, DOI 10.1074/jbc.M112.400416

Thomas O. Eichmann[‡], Manju Kumari[‡], Joel T. Haas[§], Robert V. Farese, Jr.[§], Robert Zimmermann[‡], Achim Lass[‡1], and Rudolf Zechner[‡2]

From the [‡]Institute of Molecular Biosciences, University of Graz, 8010 Graz, Austria and [§]Gladstone Institute of Cardiovascular Disease and Departments of Medicine and Biochemistry and Biophysics, University of California, San Francisco, California 94141

Background: Adipose triglyceride lipase (ATGL) degrades triacylglycerol to diacylglycerol (DAG). The stereo/regioselectivity of ATGL is unknown.
Results: ATGL specifically generates *sn*-1,3 and, in the presence of its co-activator CGI-58, *sn*-1,3 and *sn*-2,3 DAG.
Conclusion: ATGL generates distinct DAG isoforms that cannot directly enter phospholipid synthesis or activate protein kinase C.
Significance: Elucidation of the stereo/regioselectivity of ATGL is crucial to understand cellular DAG metabolism and signaling.

Adipose triglyceride lipase (ATGL) is rate-limiting for the initial step of triacylglycerol (TAG) hydrolysis, generating diacylglycerol (DAG) and fatty acids. DAG exists in three stereochemical isoforms. Here we show that ATGL exhibits a strong preference for the hydrolysis of long-chain fatty acid esters at the *sn*-2 position of the glycerol backbone. The selectivity of ATGL broadens to the *sn*-1 position upon stimulation of the enzyme by its co-activator CGI-58. *sn*-1,3 DAG is the preferred substrate for the consecutive hydrolysis by hormone-sensitive lipase. Interestingly, diacylglycerol-*O*-acyltransferase 2, present at the endoplasmic reticulum and on lipid droplets, preferentially esterifies *sn*-1,3 DAG. This suggests that ATGL and diacylglycerol-*O*-acyltransferase 2 act coordinately in the hydrolysis/re-esterification cycle of TAGs on lipid droplets. Because ATGL preferentially generates *sn*-1,3 and *sn*-2,3, it suggests that TAG-derived DAG cannot directly enter phospholipid synthesis or activate protein kinase C without prior isomerization.

Essentially all organisms depend on fatty acids (FAs)[3] as energy substrates and precursors for the synthesis of membrane and signaling lipids. Accordingly, all cells of multicellular organisms must have access to a constant supply of FAs. Because of their amphipathic properties, however, high cellular concentrations of unesterified FAs must be avoided because they cause cell damage and dysfunction ("lipotoxicity"). To assure sufficient FA supply without provoking the harmful impact of elevated cellular FA concentrations, they are esterified with glycerol to form chemically inert triacylglycerol (TAG). All cells with high FA demand can store TAG in cytosolic lipid droplets (LDs). Higher animals additionally possess white adipose tissue (WAT), which is specialized to deposit large amounts of fat and to provide the whole organism with FAs upon demand. Within LDs, TAGs constitute the hydrophobic core, which is coated by a monolayer of phospholipids and structural proteins such as the perilipins (1).

The release of FAs from LD-associated TAG is mediated by TAG hydrolases commonly called "lipases." Studies with induced mutant mouse models (2–5) and patients with "neutral lipid storage disease" (6, 7) revealed that in mammals hydrolysis of cellular TAG (lipolysis) involves at least three lipases that act in a consecutive manner. Adipose triglyceride lipase (ATGL) catalyzes the initial, rate-limiting step by converting TAG to diacylglycerol (DAG) (8). In the second step DAG is hydrolyzed by hormone-sensitive lipase (HSL). Although HSL can also hydrolyze TAG to some extent, the main lipolytic function of the enzyme *in vivo* is DAG hydrolysis (8, 9). The product of the HSL reaction is monoacylglycerol (MAG), which is subsequently hydrolyzed by monoglyceride lipase (MGL) (10). Hor-

* This work was supported by the grant "GOLD: Genomics Of Lipid-associated Disorders," which is part of the Austrian Genome Project "GEN-AU: Genome Research in Austria" funded by the Austrian Ministry of Science and Research and the Austrian Research Promotion Agency. This work was also supported by the Grants P21296, F30 SFB LIPOTOX, the Doktoratskolleg W901-B05DK (Molecular Enzymology), and the Wittgenstein Award Z136, which are funded by the Austrian Science Fund. Additional funding was obtained from the City of Graz and the Province of Styria.

[1] To whom correspondence may be addressed: Institute of Molecular Biosciences, University of Graz, Heinrichstrasse 31, 8010 Graz, Austria. Tel.: 43-316-380-1900; Fax: 43-316-380-9016; E-mail: achim.lass@uni-graz.at.

[2] To whom correspondence may be addressed: Institute of Molecular Biosciences, University of Graz, Heinrichstrasse 31, 8010 Graz, Austria. Tel.: 43-316-380-1900; Fax: 43-316-380-9016; E-mail: rudolf.zechner@uni-graz.at.

[3] The abbreviations used are: FA, fatty acid; ATGL, adipose triglyceride lipase; BSSL, bile-salt stimulated lipase; CGI-58, comparative gene identification-58; CPT, CDP-choline:1,2-diacylglycerol cholinephosphotransferase; DAG, diacylglycerol; DAGL, diacylglycerol lipase; DGAT, diacylglycerol-O-acyltransferase; DGK, diacylglycerol kinase; ER, endoplasmic reticulum; FAME, fatty acid methylester; FFA, free fatty acid; GL, gastric lipase; HSL, hormone-sensitive lipase, LacZ, beta-galactosidase; LD, lipid droplet; LL, lingual lipase; LPL, lipoprotein lipase; MAG, monoacylglycerol; MGL, monoglyceride lipase; PLC, phospholipase C; PKC, protein kinase C; PL, pancreatic lipase; PNPLA, patatin-like phospholipase domain containing; RT, room temperature; sn, stereospecific numbering; TAG, triacylglycerol; TLC, thin layer chromatography; WAT, white adipose tissue.

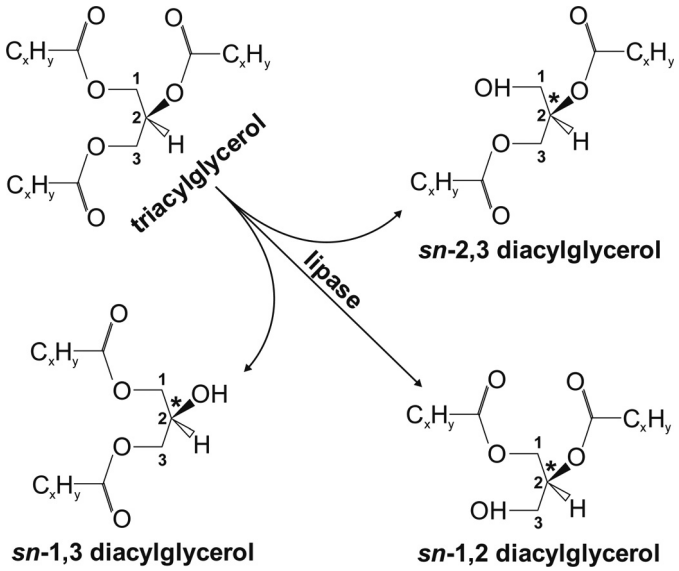

FIGURE 1. **Schematic depiction of enzymatic TAG hydrolysis and formation of potential DAG products.** Hydrolysis of the prochiral TAG may lead to formation of the regioisomer *sn*-1,3 DAG upon cleavage of the *sn*-2 position or to the enantiomers *sn*-1,2 or *sn*-2,3 DAG by hydrolysis of the ester bond at the *sn*-3 or *sn*-1 position, respectively. The numbers denoted on the carbon atoms of the glycerol backbone indicate the *stereospecific numbering* (*sn*). The *asterisk* indicates the chiral center of the DAG at the *sn*-2 position.

monal stimulation of lipolysis by *e.g.* β-adrenoreceptor agonists leads to the activation of ATGL by comparative gene identification 58 (CGI-58) (11, 12), phosphorylation, and translocation of HSL to LDs, resulting in the efficient catabolism of TAGs to glycerol and three FAs (13).

According to the chemical structure of TAGs, lipases exhibit unique stereoselectivity on encountering prochiral and chiral substrates. This distinguishes them from other hydrolases, such as proteases, phospholipases, or nucleases, which encounter only one optical antipode of their substrates (14). TAGs comprise both chiral and prochiral molecules depending on the composition of the FAs, which are esterified to the glycerol backbone. Triolein, for example, with three oleic acids esterified to its glycerol backbone, is thus a prochiral molecule. Upon hydrolysis of either the *sn*-1 or *sn*-3 position, it transforms to the chiral, enantiomeric molecules *sn*-2,3 or *sn*-1,2 diolein, respectively, whereas hydrolysis of the *sn*-2 position leads to the regioisomeric form *sn*-1,3 diolein (Fig. 1). The ability of lipases to recognize and differentiate between chiral and prochiral substrates raises questions concerning the impact of their stereo/regioselectivity as well as the stereochemistry of their products. A variety of animal and microbial TAG lipases have been studied for their stereoselectivity; the large majority of them showed *sn*-1 or *sn*-3 selectivity (14). Only very few microbial lipases catalyze the hydrolysis of the secondary ester bond at the *sn*-2 position, and only the *Candida antarctica* A lipase exhibited clear positional selectivity for the *sn*-2 position, suggesting that most lipases are *sn*-1- or *sn*-3-specific (14).

The stereo/regioselectivity of TAG hydrolysis is highly relevant for subsequent reactions and biological activities of the resulting DAG. First, *sn*-1,2 DAG is a substrate for glycerophospholipid biosynthesis, whereas *sn*-1,3 or *sn*-2,3-DAG is not. Second, *sn*-1,2 DAG but not the other two isomers are potent activators of protein kinase C (15–17), thereby regulating numerous pathways of cell growth and metabolism. Third, DAG can be re-esterified to TAG by diacylglycerol-*O*-acyltransferases (DGATs), and it is currently not clear which DAG isomers are preferred substrates for DGAT1 or DGAT2.

In this study we investigated the FA species and stereo/regioselectivity of ATGL. Our results indicate that the enzyme efficiently hydrolyzes C:16 and C:18 FA esters with a slight substrate preference for palmitoleic acid (C16:1). Importantly, ATGL has a strong preference for the hydrolysis of FA esters at the *sn*-2 position of the glycerol backbone. This selectivity broadens in the additional presence of the ATGL co-activator CGI-58, resulting in the formation of *sn*-1,3 and *sn*-2,3 DAG. ATGL/CGI-58 does not generate detectable amounts of *sn*-1,2 DAG, suggesting that the ATGL reaction product cannot directly be utilized for glycerophospholipid synthesis or PKC activation. In contrast, the ATGL reaction products and particularly *sn*-1,3 DAG are preferred substrates for HSL-mediated degradation and re-esterification by DGAT2.

EXPERIMENTAL PROCEDURES

Materials—Chemicals and radiochemicals were obtained from Sigma and GE Healthcare, respectively. Lipids were supplied by Larodan Fine Chemicals (Malmō, Sweden; TAGs), Avanti Polar Lipids (Alabaster, AL; phospholipids) or Sigma (DAGs).

Animals—Mice (C57Bl/6) were housed on a regular light/dark cycle (12 h/12 h) and had *ad libitum* access to water and normal chow diet (4.5% w/w fat; Ssniff, Soest, Germany). 8–10-week-old male mice were used for studies. Mice with a global deletion of HSL (HSLko) or ATGL (ATGLko) were generated as described previously (3, 4). Blood and WAT of fed and 8-h-fasted animals were used for lipid analyses. Blood was collected from isoflurane-anesthetized mice (Baxter, Deerfield, IL) via retro-orbital puncture. WAT samples were surgically removed from cervically dislocated mice. Tissue samples were washed in ice-cold phosphate-buffered saline (PBS) containing 1 mM EDTA, 100 IU/ml heparin, and disrupted using an Ultra Turrax® (IKA, Staufen, Germany) either in ice-cold solution A (0.25 M sucrose, 1 mM EDTA, 1 mM DTT, 20 μg/ml leupeptin, 2 μg/ml antipain, and 1 μg/ml pepstatin, pH 7.0) for enzymatic activity measurements or in methanol for lipid extraction and analyses.

cDNA Cloning of Recombinant Proteins—pcDNA4/HisMaxC vector (Invitrogen) constructs containing the entire open reading frame of murine ATGL, murine CGI-58, and murine HSL were generated as described previously (18). Constructs of FLAG-tagged DGAT1 and DGAT2 were generated as described (19). For expression and subsequent purification of CGI-58, the coding sequence was subcloned into pYex4T-1 vector (Clontech Laboratories Inc., Mountain View, CA) as described previously (11).

Purification of GST-tagged CGI-58—GST-tagged CGI-58 was expressed in *Saccharomyces cerevisiae* BY4742 strain and purified as described (11).

Expression of Recombinant Proteins—SV-40 transformed monkey embryonic kidney cells (Cos-7; ATCC, CRL-1651) were cultivated in DMEM (Invitrogen) with 10% fetal calf

serum (FCS; Sigma) supplemented with penicillin (100 IU/ml) and streptomycin (100 μg/ml) at standard conditions (95% humidified atmosphere, 37 °C, 5% CO_2). Cells were transfected with 1 μg of recombinant DNA complexed with Metafectene (Biontex, Munich, Germany) in FCS-free medium. After 4 h, the medium was changed to DMEM containing 10% FCS. Finally, after 48 h, cells were washed twice with PBS and collected using a cell scraper.

Preparation of Tissue and Cell Homogenates—Cells were disrupted in solution A by sonication using a Virsonic 475 (Virtis, Gardiner, NJ). Both cell and tissue homogenates were centrifuged to remove nuclei and unbroken cells (1,000 × *g*, 4 °C, 30 min). For membrane-free cytosolic fractions, homogenates were further centrifuged (100,000 × *g*, 4 °C, 60 min). The microsomal pellet was resuspended in ice-cold solution A to obtain the microsomal fraction.

Protein Determination—Protein concentrations of total cell homogenates and cellular fractions were determined using Bio-Rad protein assay reagent (Bio-Rad). Bovine serum albumin (BSA) served as the standard.

Immunoblotting—Homogenates of transfected Cos-7 cells (20–30 μg of protein) or WAT microsomal fractions (20–30 μg of protein) were subjected to SDS-PAGE and blotted onto PVDF membranes (Carl Roth GmbH, Karlsruhe, Germany) by standard methodology. His- or FLAG-tagged proteins (His tag: ATGL, CGI-58, LacZ, and HSL; FLAG tag: DGAT1 and DGAT2) were detected using primary anti-His or anti- FLAG antibodies and anti-mouse HRP-linked secondary antibody (GE Healthcare). Endogenous expression of DGAT1 and DGAT2 in murine WAT was detected using polyclonal DGAT1 or DGAT2 primary antibodies (ProSci, Poway, CA) and anti-rabbit HRP-linked secondary antibody (Vector Laboratories Inc., Burlingame, CA). Chemiluminescence was induced by an ECLplus kit (GE Healthcare) and detected by exposure to x-ray film.

Total Lipid Extraction and Separation—Lipids of homogenized tissue samples or blood were supplemented with 20 μg of C17:0 and 20 μg of tri-margarinate per ml as internal standards. Total lipids were extracted using chloroform/methanol/water (2/1/0.6, v/v/v, 1% acetic acid). Extraction was performed under steady shaking for 1 h at room temperature (RT). After centrifugation (1000 × *g*, 4 °C, 15 min), the organic phase was collected, dried under nitrogen, and dissolved in 500 μl of chloroform. Aliquots (30 μl) were separated by thin-layer chromatography (TLC). For TAG and FA separation, hexane/diethyl ether/acetic acid (70:29:1, v/v/v) was used as a solvent, and for DAG separation chloroform/acetone/acetic acid (95:4:1, v/v/v) was used as a solvent. TLC plates were stained with iodine vapor, and bands corresponding to selected lipid species were scraped off. For the determination of FA composition (by GC-flame ionization detection, see below), lipids were dissolved in 500 μl of toluene containing 500 μg of butylated hydroxytoluene (1 mM in toluene) as an antioxidant. For HPLC lipid analysis (see below), lipids were re-extracted with chloroform.

Fatty Acid Determination by Gas Chromatography (GC) Using a Flame Ionization Detector—FA species were analyzed by GC-flame ionization detection according to Sattler *et al.* (20) with the following modifications. For transesterification, 2 ml of BF_3 were added to lipids dissolved in 500 μl of toluene and incubated for 1 h at 110 °C. Reactions were stopped by the addition of 1 ml of ice-cold H_2O. FA methyl esters (FAMEs) were extracted twice by the addition of 2 ml of hexane/chloroform (4:1, v/v) and shaking for 10 min at RT. After centrifugation (1000 × *g*, 10 min, RT) the upper phase was collected. The combined phases were evaporated under nitrogen, and FAMEs were dissolved in 100 μl of hexane. The GC conditions were set to split injection (split flow, 15 ml/min; split ratio, 1/5; injection volume, 2 μl) using an injector temperature of 230 °C and a wall-coated open tubular fused silica column (25 m, 0.32-mm inner diameter, free fatty acid phase-coated, film thickness = 0.3 μm; Agilent Technologies, Santa Clara, CA). The carrier gas consisted of helium. As a temperature gradient, two consecutive ramps from 150 to 260 °C (ramp 1, 5 °C/min to 250 °C hold for 2 min; ramp 2, 10 °C/min to 260 hold for 5 min) were used. Flame ionization detector (Trace-GC 2000series, ThermoQuest Corp., Atlanta, GA) conditions were as follows: base temperature, 150 °C; gas flow, 200 ml/min air, 30 ml/min hydrogen, and 20 ml/min helium. Data acquisition and analysis were done with Xcalibur 2.0 software (Thermo Fisher Scientific, Waltham, MA). For quantitative analysis the corresponding peaks of FAMEs were integrated, and peak areas were calculated in relation to the C17:0 peak as the internal standard. FAME concentrations were calculated as percentage of total FAMEs in a given sample and/or as amounts per wet tissue weight (nmol/g).

Enzymatic Generation of DAG—The triolein substrate (0.3 mM) containing 1.0×10^6 cpm [^{3}H]triolein (9, 10) as tracer (per sample) and 45 μM phosphatidylcholine was emulsified on ice in 100 mM potassium phosphate buffer, pH 7.0, using a sonicator (Virsonic 475, VirTis, Gardiner, NY). Then the substrate was adjusted to 5% BSA (FA-free), and 100 μl of substrate were incubated with cytosolic fractions of Cos-7 cell lysates (50 μg of protein) overexpressing ATGL. Incubations were performed in the presence or absence of 200 ng of purified CGI-58-GST and/or HSL-specific inhibitor (12.5 μM 76-0079; Novo Nordisk, Copenhagen, Denmark), respectively, in a water bath at 37 °C for either 60 or 120 min. The reaction was terminated by extracting the lipids according to Folch *et al.* (21). Subsequently, lipids were separated by TLC using chloroform/acetone/acetic acid (95/4/1, v/v/v) as solvent. Then, bands corresponding to DAG were scraped off, and the radioactivity was determined by liquid scintillation counting (Tri-Carb 2300 TR; PerkinElmer Life Sciences). Alternatively, lipids were re-extracted from the silica using chloroform and used for further analyses.

Determination of Hydrolase Activity—TAG or DAG substrates were prepared by emulsification of either 0.25 mM TAG or 0.3 mM DAG with 45 μM phosphatidylcholine in 100 mM potassium phosphate buffer, pH 7.0, on ice using a sonicator (Virsonic 475). 100 μl of substrate were incubated with 50 μg of protein of Cos-7 cell homogenates overexpressing various lipases, and 50 μg of protein of Cos-7 cell homogenates overexpressing CGI-58 or LacZ (total volume, 200 μl) in a water bath at 37 °C for 60 min. Then 200 μl of 0.1% Triton X-100 were added, and samples were agitated for 10 min at RT. The

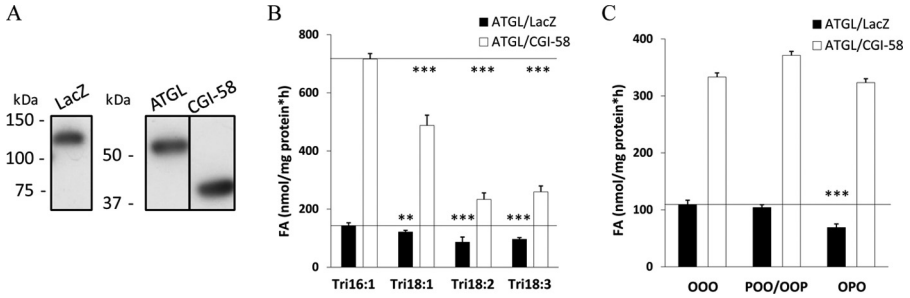

FIGURE 2. **ATGL hydrolyzes TAGs with FAs of different chain length and saturation *in vitro*.** *A*, recombinant proteins were expressed in Cos-7 cells, and expression of His-tagged proteins was assessed by immunoblotting. *B* and *C*, homogenates of Cos-7 cells overexpressing ATGL were incubated in the absence or presence of CGI-58 with different, homogeneously (*B*) or heterogeneously esterified TAG species (*C*) as substrates for 1 h at 37 °C. Released FAs were measured using a NEFA-C kit. Data are normalized to LacZ and presented as the means ± S.D. and are representative of two independent experiments (***, $p < 0.001$; **, $p < 0.01$). *O* = oleic acid, C18:1; *P* = palmitic acid, C16:0.

released FAs were determined using a NEFA-C kit (Wako Chemicals, Neuss, Germany).

Determination of DGAT Activity—Various DAG substrates were incubated in a final volume of 100 μl with 50 μg of protein of cellular homogenates or WAT microsomal fraction in the presence of HSL inhibitor (12.5 μM, 76-0079, Novo Nordisk), orlistat (25 μM, Xenical®), and in the presence or absence of a DGAT1 inhibitor (5 μM) (22). DAG substrates were emulsified by sonication (Virsonic 475) and contained 0.2 mM DAG (*sn*-1,2-, *sn*-1,3-, or *rac*-1,2/2,3 diolein) in Tris buffer (50 mM, 20 mM $MgCl_2$, pH 7.4) and 0.8 mM phosphatidylcholine. After sonication, oleoyl-CoA and [^{14}C]oleoyl-CoA (55 μCi/μmol) were added to a final concentration of 30 and 20 μM, respectively. The substrate was mixed 1:1 (v:v) with the samples to give a final volume of 200 μl and incubated for 10 min at RT. Reactions were stopped by lipid extraction with chloroform/methanol (2:1, v/v). Lipid extracts were separated by TLC using hexane/diethyl ether/acetic acid (70/29/1, v/v/v) as solvent. TLC bands corresponding to TAG were scraped off, and radioactivity was determined by liquid scintillation counting (Tri-Carb 2300 TR).

Acylglycerol Determination—Acylglycerol content (TAG, DAG, MAG, and glycerol) of lipid extracts from tissue preparations as well as different nonradiolabeled TAG substrates were determined using an INFINITY Triglyceride kit (Thermo Scientific Fisher, Middletown, VA). Lipids from tissue preparations as well as substrates were measured directly, whereas lipids from TLC bands were first extracted with chloroform, then diluted 1:1 with 0.1% Triton X-100 and measured.

Enzymatic Hydrolysis of Lecithin—5 mg of lecithin (egg yolk, average molecular weight ~800 g/mol; Sigma) were emulsified in 10 ml of potassium phosphate buffer (100 mM, pH 7.4) by sonication (Virsonic 475). 500 μl of lipid emulsion (~0.7 mM) was incubated with 100 μl of recombinant phospholipase C (PLC, *Bacillus cereus*, 100 IU/ml; Sigma) for 2 h at 37 °C. Lipids were extracted according to Folch *et al.* (21) and separated by TLC using chloroform/acetone/acetic acid (95/4/1, v/v/v) as solvent. Bands corresponding to DAG were scraped off, re-extracted with chloroform, and subjected to chiral-phase HPLC analysis.

Determination of DAG Isomers by Chiral Phase HPLC—DAG isolates of various sources were dried under nitrogen and derivatized according to Itabashi *et al.* (23) with slight modifications. In short, DAGs were dissolved in 400 μl of dry toluene and 40 μl of pyridine. After the addition of 2 mg of 3,5-dinitrophenylisocyanate, the reaction mixture was shaken for 1 h at RT, dried under nitrogen, and dissolved in chloroform. Subsequently, the reaction products were separated by TLC using UV_{254} silica plates (Sigma) and chloroform/methanol (95/5, v/v) as solvent. TLC bands corresponding to 3,5-dinitrophenylurethanes were visualized under UV light, scraped off, and extracted twice with chloroform. After evaporation of the solvent, samples were dissolved in 100 μl of hexane/dichloroethane/ethanol (80/20/2, v/v/v) and subjected to HPLC analysis. The HPLC system consisted of a Waters alliance e2695 separation module (Millford, MA) and a UV-visible 2489 detector. For separation, a YMC-Pack A-K03 column (YMC Inc., Kyoto, Japan) containing (*R*)-(+)-1-(1-naphtyl)ethylamine as stationary phase was used. Samples were analyzed under isocratic conditions using hexane/dichloroethane/ethanol (80/20/2, v/v/v; flow rate, 1 ml/min) as the mobile phase. DAG derivatives were detected at 226 nm. Peaks corresponding to DAG species were integrated and expressed as the percentage of total DAG using Empower pro software (Waters).

Statistics—Data are shown as the means ± S.D. Statistical significance between two groups was determined by unpaired Student's two-tailed *t*-test. The following levels of statistical significance were used: *, $p < 0.05$; **, $p < 0.01$; ***, $p < 0.001$.

RESULTS

ATGL Hydrolyzes Long Chain FA Esters—To investigate the FA selectivity of ATGL, we expressed murine ATGL and CGI-58 in Cos-7 cells (Fig. 2*A*) and performed TAG hydrolase activity assays using different TAG species as substrates. In the first set of experiments, TAG substrates contained identical FAs in all three ester bonds with glycerol. The high melting point (>40 °C) of TAG uniformly esterified with saturated FAs (C12:0, C14:0, C16:0, C18:0) precluded the preparation of suitable lipid emulsions. Therefore, uniformly esterified TAG substrates with C16:1, C18:1, C18:2, and C18:3 were tested and used at saturating substrate concentrations. Among these, ATGL showed the highest activity for tripalmitolein (Fig. 2*B*) followed by triolein, trilinolenin, and trilinolein. The same result was observed when ATGL was co-activated by CGI-58. Despite a significant decline of ATGL substrate selectivity with increasing FA chain length and desaturation (C16:1 *versus* C18:2

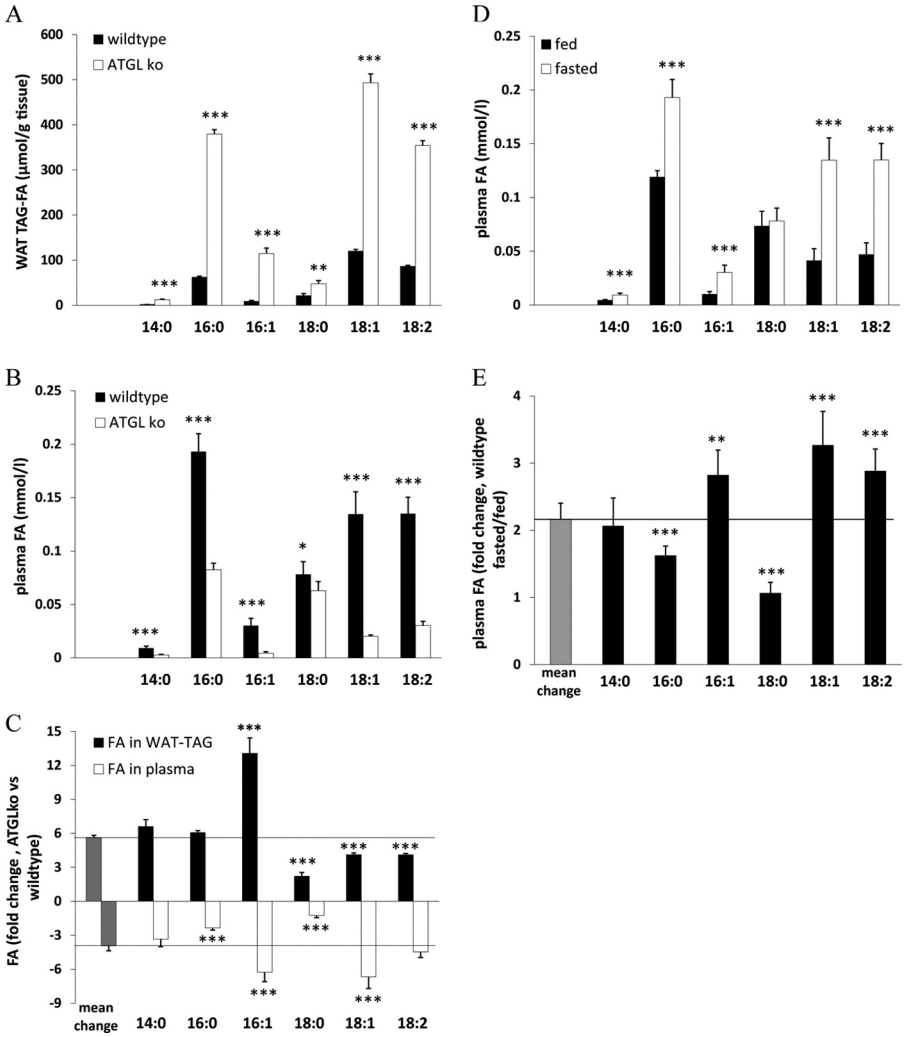

FIGURE 3. **ATGL exhibits a preference for unsaturated FAs *in vivo*.** *A*, WAT lipids of fed wt and ATGLko mice were extracted according to Folch *et al.* (21) and separated by TLC. TAGs were isolated and transesterified. FAMEs were separated and analyzed using GC/ flame ionization detector. *B*, plasma lipids of overnight-fasted wt and ATGLko mice were extracted and analyzed as in *A*. *C*, numeric changes in FA species of WAT TAGs and plasma FAs from wt and ATGLko mice are shown. *D*, plasma lipids of fed and overnight-fasted wt mice were extracted and analyzed as in *A*. *E*, numeric changes in plasma FA species of fed and fasted wt mice are shown. Data are presented as the means ± S.D. and are representative of two independent experiments (***, $p < 0.001$; **, $p < 0.01$; *, $p < 0.05$). $n = 4$ (each genotype).

for ATGL, −47%; for ATGL/CGI-58, −69%), the enzyme was highly active and activatable by CGI-58 with all four substrates.

Next, we determined whether ATGL exhibits a preference for the degree of desaturation of FA esterified at different stereochemical positions of the glycerol backbone. Compared with triolein as substrate, ATGL and ATGL/CGI-58 hydrolyzed triglyceride substrates with two oleic acids and one palmitic acid either on the *sn*-2 or *rac*-1/3 position with comparable rates, indicating that ATGL hydrolyzes saturated and monounsaturated FAs with similar efficiency *in vitro* (Fig. 2*C*).

ATGL Hydrolyzes Long-chain FA Esters in Vivo with a Modest Substrate Preference for C16:1—To assess FA preference of ATGL *in vivo*, we examined FA profiles of WAT-TAGs from fed wild-type (wt) and ATGLko mice. Additionally, we determined net plasma FA composition of 8-h-fasted wt and ATGLko mice. The FA composition of WAT-TAG differed significantly between wt and ATGLko mice. Normalized to tissue weight, all FA species in TAGs increased in WAT of ATGLko mice, with the most pronounced increase in palmitoleic acid (13-fold) (Fig. 3*A*). Conversely, the lipolytic defect decreased the occurrence of unesterified FAs in plasma after fasting. The most pronounced reductions were observed for palmitoleic acid (-85%), oleic acid (-85%), and linoleic acid (−78%) (Fig. 3*B*). The calculated relative changes in WAT-TAG FAs and plasma unesterified FAs revealed a moderate preference of ATGL for unsaturated FAs, in particular for palmitoleic acid (Fig. 3*C*). To test whether the ATGL-dependent release of specific FA species can also be observed in wt mice during fasting periods, we compared the plasma FA composition of fed and 8-h-fasted wt mice. Fasting led to a pronounced increase (3-fold) in the plasma concentration of unsaturated FAs (C16:1, C18:1, and C18:2) (Fig. 3, *D* and *E*). Together, these *in vitro* and *in vivo* data demonstrate that (i) ATGL is able to hydrolyze glycerol ester bonds of all major long-chain FAs, (ii) in mice, ATGL exhibits a tendency to preferred cleavage of esters with mono- or polyunsaturated FAs, and (iii) the blunted plasma FA release in fasted ATGLko mice suggests that ATGL activity is instrumental for increased lipolysis during fasting.

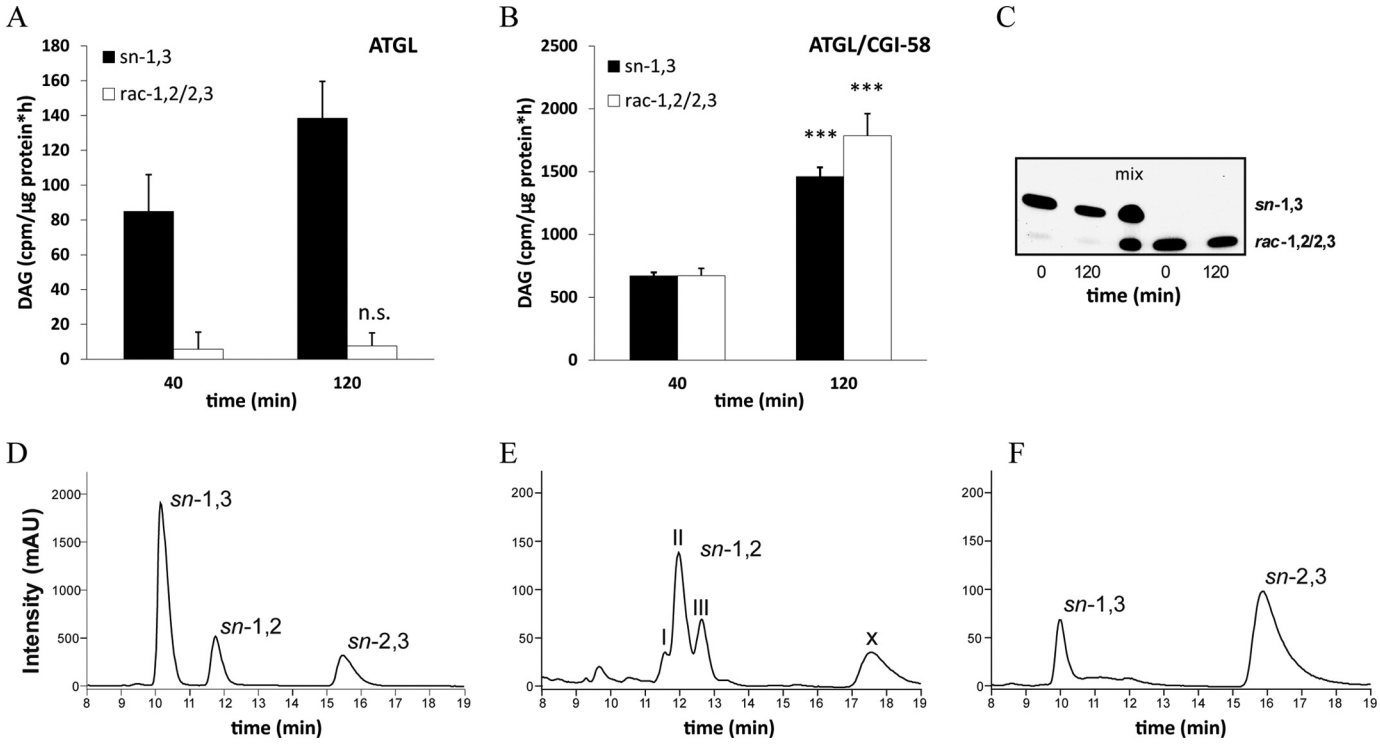

FIGURE 4. **ATGL specifically cleaves the *sn*-2 ester bond and expands its selectivity to the *sn*-1 position upon co-activation by CGI-58.** *A* and *B*, cytosolic fractions of Cos-7 cells overexpressing ATGL were incubated in the absence (*A*) or presence (*B*) of GST-tagged CGI-58 with ^{3}H-labeled triolein substrate in the presence of an HSL-specific inhibitor (76-0079) at 37 °C. Reactions were stopped at different time points, DAG regioisomers were separated by TLC, and radioactivity in the corresponding bands was measured by liquid scintillation counting. *n.s.*, not significant. *C*, to assess transesterification of DAG isomers, *sn*-1,3 and *rac*-1,2/2,3 DAG were incubated with lysates of Cos-7 cells in the presence of an HSL-specific inhibitor (76-0079) for 120 min at 37 °C. DAG species were analyzed by TLC before and after incubation. *D*--*F*, chiral-phase HPLC resolution of different DAG species is shown. DAGs were analyzed as their corresponding 3,5-dinitrophenylurethanes by chiral-phase HPLC. Analysis of a racemic diolein reference mix is shown in *D*. Analysis of the reaction products of "egg yolk lecithin" hydrolyzed by purified PLC (*B. cereus*) is shown. The three peaks within the retention time range 11.5–13 min display the different FA composition of the separated DAGs; I, 16:0–18:1 + 18:1–18:1; II, 16:0–18:2 + 18:1–18:2; III, 18:2–18:2 (*E*). Analysis of the reaction products of triolein substrate hydrolyzed by CGI-58 co-activated ATGL contained in the cytosolic fraction of Cos-7 cells and in the presence HSL-specific inhibitor (76-0079, *F*). Data are normalized to LacZ and are presented as the means ± S.D. and are representative of two independent experiments (***, $p < 0.001$). *X* = unknown compound. *mAU*, milliabsorbance units.

ATGL Is Selective for the sn-2 Position of TAG and Generates sn-1,3 DAG—To investigate whether ATGL exhibits positional selectivity for TAG hydrolysis, we incubated cytosolic fractions of Cos-7 cells overexpressing ATGL with ^{3}H-labeled triolein for different time periods and measured DAG formation. To exclude the contribution of TAG hydrolysis by HSL, all incubations were performed in the presence of a potent HSL inhibitor (76-0079). The presence of ATGL without CGI-58 led to the predominant generation of *sn*-1,3 DAG (Fig. 4*A*). Over an incubation period of 120 min, the *sn*-1,2 or *sn*-2,3 DAG enantiomers were hardly detectable and showed no increase with the duration of incubation (Fig. 4*A*).

ATGL Co-activated by CGI-58 Additionally Generates sn-2,3 DAG—The addition of recombinant CGI-58 to the assay led to time-dependent formation of *rac*-1,2/2,3 DAG (Fig. 4*B*). After an incubation of 120 min, approximately equal amounts of *sn*-1,3 DAG and *rac*-1,2/2,3 DAG were present. Thus, ATGL without co-activator is highly specific for the hydrolysis of *sn*-2 esters and broadens its selectivity to *sn*-1 or *sn*-3 esters upon CGI-58 co-activation. Clarification of the stereoselectivity of ATGL upon CGI-58 co-activation required the distinction between *sn*-1,2 DAG and *sn*-2,3 DAG. Therefore, we applied chiral-phase HPLC to facilitate separation of all three DAG isomers (23). TAG emulsions were hydrolyzed with ATGL in the presence of CGI-58 using non-labeled triolein as substrate. Subsequently, DAGs were isolated and converted to their corresponding 3,5-dinitrophenylurethane derivatives, which were amenable to chiral-phase HPLC analysis. For validation of the method, we analyzed a commercially available racemic diolein reference sample. In the chromatogram, all three DAG species showed distinctly separated peaks in a time range of 16 min (Fig. 4*D*). Egg yolk-lecithin digested with PLC (*B. cereus*) served as a positive control for *sn*-1,2 DAG. As expected, the PLC-dependent breakdown of lecithin generated only one DAG species, *sn*-1,2 DAGs (Fig. 4*E*), with several subpeaks due to variation in FA composition. Importantly, hydrolysis of TAG by CGI-58-co-activated ATGL led to the formation of *sn*-1,3 and *sn*-2,3 DAGs, whereas *sn*-1,2 DAG was not detectable (Fig. 4*F*). Apparently, the presence of CGI-58 extends the selectivity of ATGL from an exclusive *sn*-2 hydrolase to a *sn*-1- and *sn*-2-selective hydrolase. To determine if during prolonged incubation of DAG species any transesterification of FAs occurred, we incubated either *sn*-1,3 DAG or a racemic mixture of *sn*-1,2/2,3 DAGs with Cos-7 cell lysates under identical conditions for 120 min and determined DAG isomers by TLC. Under these experimental conditions, no indications for FA transesterification of DAG species were observable (Fig. 4*C*). Furthermore, under these conditions, also no transesterification

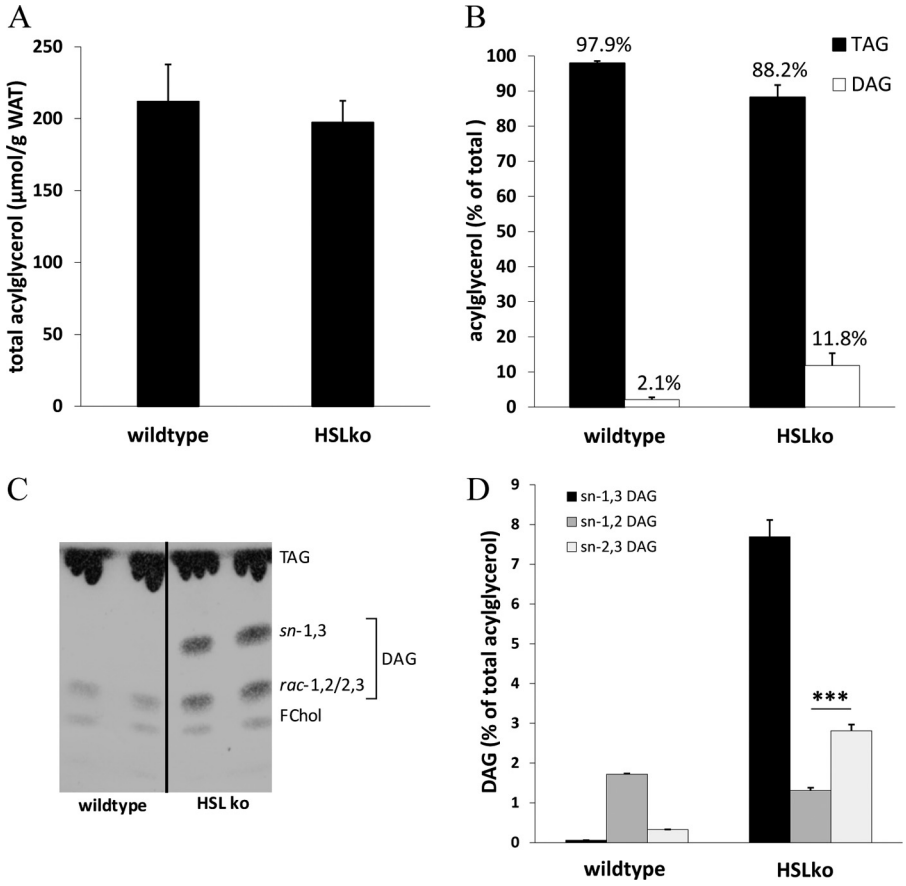

FIGURE 5. **Distinct accumulation of *sn*-1,3 DAG in WAT of HSL-deficient mice.** *A*, lipids were extracted according to Folch *et al.* (21), and total acylglycerol levels in WAT of wt and HSLko mice were determined using an Infinity-TAG kit (Thermo Scientific Fisher). *C*, neutral lipids of wt and HSL-deficient WAT were separated by TLC using chloroform/acetone/acetic acid (90/8/1; v/v/v). *B* and *D*, bands corresponding to TAG and DAG were scraped off and extracted, the acylglycerol content was determined using an Infinity-TAG kit (*B*), and DAG isomers were analyzed by chiral-phase HPLC (*D*). Data are presented as the means ± S.D. (***, $p < 0.001$), $n = 4$ (each genotype). *FChol*, free cholesterol.

between *sn*-1,2 and *sn*-2,3 DAG isomers was observed (Fig. 4, *E* and *F*).

HSLko Animals Accumulate sn-1,3 and sn-2,3 DAG in WAT—To elucidate whether our *in vitro* findings are also relevant *in vivo*, we analyzed acylglycerol concentrations and composition in WAT of HSLko mice. HSL is a crucial enzyme for the hydrolysis of DAG within the lipolytic cascade. Therefore, HSLko mice represent a model for defective DAG hydrolysis. Confirming previous results (2, 3), total acylglycerol levels were unaltered in HSLko mice (Fig. 5*A*), but DAG concentrations were drastically increased compared with wt littermates (5-fold) (Fig. 5*B*). DAG accumulation was accompanied by a moderate reduction in tissue TAG content (Fig. 5*B*). DAG accumulation was readily detectable in TLC analyses and consisted of *sn*-1,3 DAGs and *rac*-1,2/2,3 DAGs (Fig. 5*C*). In comparison, DAGs in wt mice are barely detectable and comprise only *rac*-1,2/2,3 DAG but not *sn*-1,3 DAG.

DAGs from WAT of both genotypes were also analyzed by chiral-phase HPLC (Fig. 5*D*). In wt WAT, the total amount of cellular DAG levels was low, and the predominant isoform was *sn*-1,2 DAG (Fig. 5*D*, *left bars*). Because it is unlikely that lipolytic intermediates accumulate in wt WAT, we assume that the observed *sn*-1,2 DAGs derive from *de novo* glycerolipid synthesis. In HSLko WAT, instead, the lipolytic defect in DAG hydrolysis caused a dramatic increase in *sn*-1,3 and *sn*-2,3 DAGs,

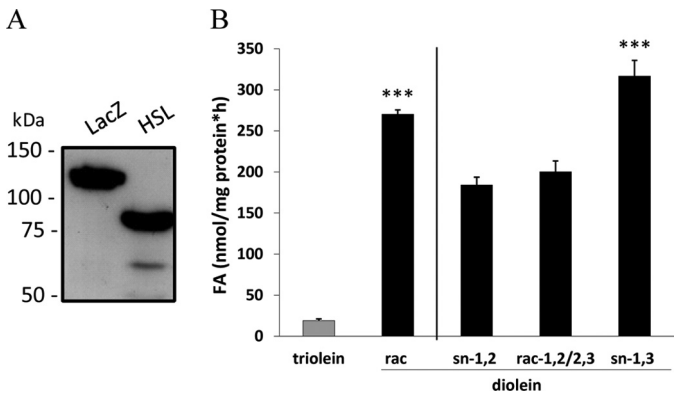

FIGURE 6. **HSL hydrolyzes all isoforms of DAG.** *A*, immunoblot analysis of lysates from Cos-7 cells expressing HSL or, as a control, LacZ using anti-His antibody is shown. *B*, lysate of Cos-7 cells expressing HSL were incubated with triolein or stereochemically different diolein substrates emulsified with phospholipids at 37 °C for 1 h. Generated FAs were measured using a NEFA-C kit (Wako Chemicals). Data are normalized to LacZ and presented as the means ± S.D. and are representative of two independent experiments (***, $p < 0.001$).

whereas the level of *sn*-1,2 DAG remained similar as in wt WAT (Fig. 5*D*, *right bars*). This increase in *sn*-1,3 and *sn*-2,3 DAGs in WAT of HSLko mice provides strong *in vivo* evidence that ATGL/CGI-58 preferably hydrolyzes *sn*-1 and *sn*-2 ester bonds but not *sn*-3 ester bonds in TAG and is consistent with our *in vitro* findings.

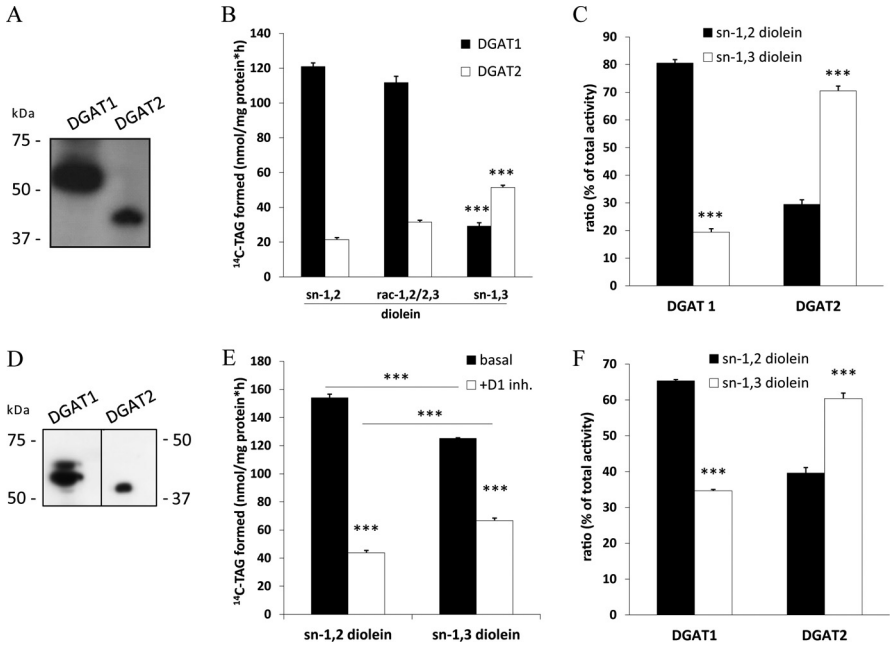

FIGURE 7. **DGAT1 and DGAT2 exhibit different preferences for DAG regioisomers.** *A*, expression of FLAG-tagged murine DGAT1 and DGAT2 in Cos-7 cells was assessed by immunoblotting. *B*, lysates of Cos-7 cells expressing FLAG-tagged DGAT1 or DGAT2 were incubated with either *sn*-1,2, *rac*-1,2/2,3, or *sn*-1,3 diolein substrate emulsified with phospholipids and ^{14}C-labeled oleoyl-CoA at 37 °C for 10 min. Lipids were extracted and separated by TLC, and radioactivity in the TAG bands was determined by scintillation counting. *C*, regioselectivity of recombinant DGAT enzymes against *sn*-1,2 or *sn*-1,3 diolein is expressed as a percentage of total acyltransferase activity. *D*, endogenous expression of DGAT1 and DGAT2 in WAT was determined by immunoblotting using anti-DGAT1 and anti-DGAT2 antibody. *E*, microsomal fractions of WAT from fed C57Bl/6-mice were assayed for DGAT activity in the presence and absence of a specific DGAT1 inhibitor (*D1 inh.*, 2-((1s,4s)-4-(4-(4-amino-7,7-dimethyl-7H-pyrimido[4,5-b][1,4]oxazin-6-yl)phenyl)cyclohexyl)acetic acid) using *sn*-1,2 or *sn*-1,3 diolein as substrate as described in *A*. *F*, regioselectivity of endogenous DGATs in WAT expressed as a percentage of total acyltransferase activity is shown. Data are normalized to LacZ and presented as means ± S.D. and are representative of two independent experiments (***, $p < 0.001$).

HSL Hydrolyzes all Isoforms of DAG—Next, we investigated the stereo/regioselectivity of HSL using lysates of Cos-7 cells overexpressing the murine enzyme (Fig. 6*A*). Assays were performed in the presence of different DAG isoforms or TAG (Fig. 6*B*). In accordance with previous work (9), HSL showed around 10-fold higher activity for racemic DAG (*rac*-1,2/2,3/1,3) than for TAG. Furthermore, HSL was able to hydrolyze all three isomers of DAG with similar efficiency.

DGAT2 but Not DGAT1 Preferentially Esterifies sn-1,3 DAG—DAG esterification is catalyzed by DGAT1 or DGAT2. To investigate the stereo/regioselectivity of these enzymes, we transfected Cos-7 cells with expression plasmids for DGAT1 or DGAT2 and used lysates containing FLAG-tagged recombinant DGAT proteins (Fig. 7*A*) in acyltransferase assays with *sn*-1,2, *sn*-1,3, or *rac*-1,2/2,3 DAG as the acyl acceptor and radiolabeled oleoyl-CoA as the acyl donor. Both DGAT enzymes were able to acylate all DAG isoforms as substrates, although with different efficiencies. DGAT1 acylated *sn*-1,2 and *rac*-1,2/2,3 DAGs 5-fold more effectively than *sn*-1,3 DAGs (Fig. 7*B*). Notably, DGAT2 showed exactly the opposite regiopreference; *sn*-1,3 DAG was acylated 2.5- and 1.7-fold more efficiently than *sn*-1,2 DAG and *rac*-1,2/2,3 DAG, respectively (Fig. 7*B*). Similar acylation rates of DGAT1 and DGAT2 for *sn*-1,2 and *rac*-1,2/2,3 DAG suggest that they do not discriminate between the two enantiomers (Fig. 7*B*). Because expression levels for DGAT enzymes were very different, we calculated selectivity quotients and found that DGAT1 acylates *sn*-1,2 and *sn*-1,3 DAG isoforms at a 4:1 ratio, whereas DGAT2 acylates the DAG isomers at a ratio of 1:2.3 (Fig. 7*C*).

To investigate whether we can confirm this selectivity for endogenously expressed DGAT enzymes, we tested microsomal fractions of WAT from wt mice using an established DGAT1 inhibitor (22). To prevent lipase-dependent TAG/DAG hydrolysis, we also added an HSL inhibitor (76-0079) and the non-selective lipase inhibitor tetrahydrolipstatin (orlistat). Immunoblotting using antibodies specific for DGAT1 and DGAT2 proved that both enzymes are expressed in the microsomal fractions of cell lysates (Fig. 7*D*). With *sn*-1,2 DAG in DGAT activity assays, DGAT1 inhibition decreased TAG formation by 75%, suggesting that the residual 25% of DGAT activity is due to DGAT2. When *sn*-1,3 DAG was used as the substrate in an identical experimental setting, total TAG formation was moderately decreased (−20%). The addition of the DGAT1 inhibitor decreased TAG formation by 50%, indicating that half of the DGAT activity is due to DGAT2 when *sn*-1,3 DAG was used as acyl acceptor (Fig. 7*E*). Calculation of the selectivity quotient for both enzymes revealed that DGAT1 preferentially acylates *sn*-1,2 DAG, whereas DGAT2 favors *sn*-1,3 DAG (Fig. 7*F*). These results demonstrate that DGAT enzymes discriminate between different DAG isoforms.

DISCUSSION

The initial step of lipolysis and the formation of DAG are catalyzed by ATGL. This enzyme belongs to a family of patatin domain-containing proteins comprising nine members in the human genome. The official annotation of ATGL is patatin-like phospholipase domain containing 2 (PNPLA2). This name derives from the fact that some members of the family have

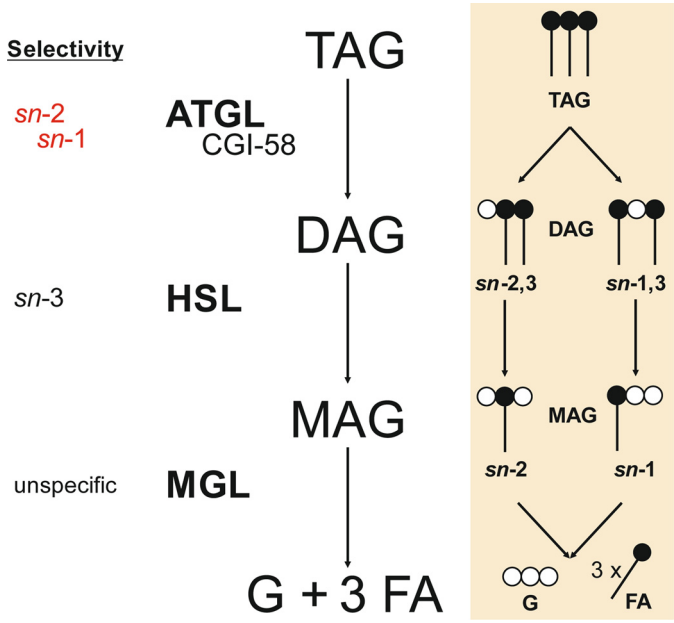

FIGURE 8. **Stereo/regioselectivity of lipolytic enzymes.** TAG is hydrolyzed to *sn*-1,3 DAG by ATGL or to *sn*-1,3 and *sn*-2,3 DAGs by ATGL co-activated by CGI-58. HSL preferentially hydrolyzes FAs at the *sn*-3 position of DAGs, yielding a mixture of MAGs (*sn*-2 and *sn*-1). MGL exhibits no selectivity in degradation of MAGs. *G*, glycerol.

potent phospholipase activities. ATGL itself is only a relatively weak phospholipase but exhibits powerful TAG hydrolase activity when co-activated by CGI-58 (11, 24). The hydrolytic catabolism of TAG stores is an essential biological process to provide FAs and other lipolytic intermediates and products in many tissues of the body. FAs are utilized as energy substrates, precursors for the synthesis of essentially all other lipid classes, and signaling molecules (13). Similarly, the intermediate TAG degradation products DAG and MAG can serve as precursors for neutral and glycerophospholipid synthesis and represent powerful signaling molecules involved in PKC and endocannabinoid signaling, respectively (25, 26). Importantly, the biological activities of DAG and MAG for lipid synthesis and signaling crucially depend on their stereochemical structure. For example, only *sn*-1,2 DAG is the precursor of glycerophospholipid synthesis (27) and is able to activate various isoforms of PKC (15–17).

In this study we investigated the substrate- and stereo/regioselectivity of ATGL by characterization of the DAG isoforms. We found that ATGL hydrolyzes long-chain, saturated, and unsaturated FAs *in vitro* and *in vivo*, with highest preference for palmitoleic acid. Furthermore, we observed that ATGL (in the absence of its co-activator CGI-58) selectively hydrolyzes TAG at the *sn*-2 position, thereby generating *sn*-1,3 DAG. This high selectivity of ATGL extends to the *sn*-1 position upon ATGL co-activation by CGI-58, resulting in the formation of *sn*-2,3 and *sn*-1,3 DAGs. Notably, ATGL does not hydrolyze *sn*-3 esters of TAG and hence does not generate detectable amounts of *sn*-1,2 DAG. The regioselectivity of ATGL alone resembles the selectivity of phospholipases within the PNPLA family. PNPLA6 and PNPLA7 act as *sn*-1 specific lyso-phospholipases, whereas PNPLA8 and PNPLA9 act as *sn*-1- and *sn*-2-specific phospholipases (28–31). The similarities in stereo/regioselectivity are consistent with the common ancestry of these enzymes. The mechanism of how CGI-58 decreases the regioselectivity of ATGL remains to be elucidated. It may, however, have an important physiological impact. It is conceivable that during basal lipolysis when ATGL is not co-activated by CGI-58, only mono- and polyunsaturated FAs from the *sn*-2 position are released. When lipolysis is activated by hormones (*e.g.* β-adrenergic receptor agonists), CGI-58 co-activates ATGL, thereby broadening its stereo/regiochemical spectrum to the *sn*-1 position, leading to higher rates of lipolysis and increased FA release for energy production.

The regioselectivity of ATGL in the absence of CGI-58 is unique in that ATGL is the only known mammalian lipase to hydrolyze TAG selectively at the *sn*-2 position. To date, all stereochemically characterized lipases involved in TAG digestion exhibit a preference for the *sn*-1 or *sn*-3 position of TAGs. Lipases of the gastrointestinal tract, including lingual lipase, gastric lipase, and pancreatic lipase, preferably hydrolyze the *sn*-3 or *sn*-1 ester bond of TAG. Additionally, they also hydrolyze the resulting DAGs, leading to the formation of MAGs and FAs (14, 32–35). Lipoprotein lipase, the major enzyme for the hydrolysis of plasma lipoprotein-associated TAG, exhibits *sn*-1 selectivity for TAG and also hydrolyzes DAG at the *sn*-2 position, generating *sn*-3 MAGs and FAs (14, 35, 36). An example of a positional unspecific lipase is bile salt-stimulated lipase, which hydrolyzes all positions of TAG, generating glycerol and FAs (37). In addition to DAGs, HSL can also catabolize TAGs *in vitro* and *in vivo* and exhibit preference for *sn*-1/3 ester bonds within TAG (9, 38).

The finding that ATGL-mediated lipolysis of TAG generates *sn*-1,3 and *sn*-2,3 DAG but apparently not *sn*-1,2 DAG makes it unlikely that lipolysis-derived DAG participates in PKC signaling. It is well established that only *sn*-1,2 DAG can activate both conventional or novel PKCs (15–17). In the classical PKC signaling pathway, *sn*-1,2 DAG is generated by the breakdown of membrane-associated phosphatidylinositol 4,5-bisphosphate by various isoforms of PLC. High cellular DAG concentrations and increased activation of specific PKC isoforms such as PKCε are strongly associated with defective insulin signaling, insulin resistance, and the pathogenesis of type 2 diabetes. In addition to PLC-mediated phospholipolysis of phosphatidylinositol 4,5-bisphosphate, *de novo* synthesis of *sn*-1,2 DAG via esterification and dephosphorylation of glycerol-3-phosphate in the endoplasmic reticulum (ER) may also contribute to the activation of certain novel PKCs (39, 40). Our results clearly demonstrate that DAGs generated during lipolysis are probably not involved in the activation of PKCs. This conclusion is also supported by the phenotype of HSLko mice. These mice accumulate large amounts of DAG in adipose and non-adipose tissues (2, 3). The fact that >90% of these acylglycerides are composed of *sn*-1,3 and *sn*-2,3 DAGs may explain why these animals do not develop a pronounced alteration in PKC signaling or insulin resistance (41–44). Although, depending on the genetic background, some HSLko strains showed signs of impaired insulin signaling (44, 45), others did not or exhibited even increased insulin sensitivity (41, 43). Also, the fact that lipolytic DAGs are generated on LDs and probably do not translocate from there to membranes precludes their involvement in PKC signaling.

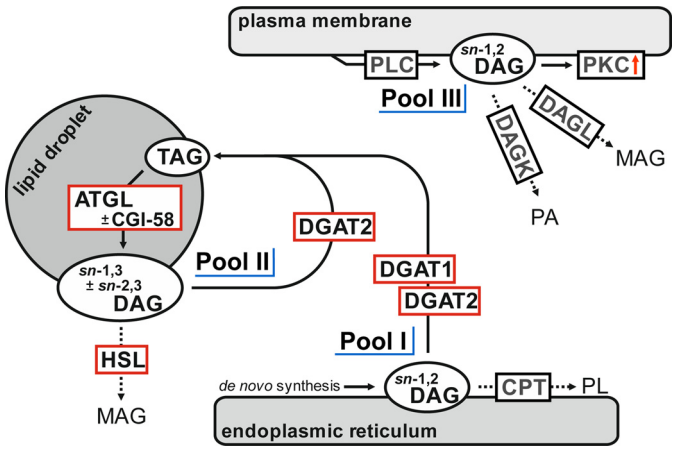

FIGURE 9. **Three-pool model of intracellular DAG distribution.** Pool I consists of *sn*-1,2 DAGs generated during *de novo* lipogenesis at the ER. DGAT1 and DGAT2 as well as CDP-choline:1,2-diacylglycerol choline phosphotransferase can metabolize newly generated *sn*-1,2 DAG. Pool II consists of *sn*-1,3 ± *sn*-2,3 DAGs, which are generated on cytosolic LDs by ATGL ± CGI-58-dependent TAG hydrolysis. Both DAG species display targets for further hydrolysis catalyzed by HSL or re-esterification catalyzed by DGAT2. *sn*-1,2 DAGs of pool III are generated by PLC at the plasma membrane and function as activators of various PKCs. Furthermore, these DAGs are substrates for DAG kinases and DAG lipases. *CPT*, choline:1,2-diacylglycerol cholinephosphotransferase; *DAGL*, diacylglycerol lipase; *DAGK*, diacylglycerol kinase; *PA*, phosphatidic acid; *PL*, phospholipid.

In addition to their signaling potential, DAGs derived from lipolysis can also be further metabolized. In cells and tissues stimulated by β-adrenergic hormones and agonists, lipolysis will continue with the hydrolysis of DAGs by HSL. HSL has been shown to hydrolyze DAGs predominantly at the *sn*-3 position (38). This stereoselectivity is consistent with the structural characteristics of the DAG substrate provided by ATGL. Results of the present study in combination with published data suggest a model of lipolysis based on stereo/regiochemical considerations (summarized in Fig. 8). ATGL cleaves the first FA at the *sn*-2 position of TAG, yielding *sn*-1,3 DAG, the preferred substrate of HSL. In stimulated lipolysis, however, ATGL co-activated by CGI-58 expands this selectivity to the *sn*-1 position, thereby generating *sn*-2,3 DAG. In accordance with our data, HSL has been shown to exhibit *sn*-3 selectivity, generating *sn*-1 and *sn*-2 MAGs (38). MGL finally catabolizes both MAGs as it does not discriminate between different MAG species (10).

Besides catabolism through lipolysis, DAGs can undergo three anabolic reactions: DAG kinases convert DAGs to phosphatidic acid, CDP-choline:1,2-diacylglycerol choline phosphotransferase converts DAG to phosphatidylcholine, and DGAT1 and -2 acylate DAG to generate TAG. The first two reactions are unlikely to occur on LDs because both DAG kinases and CDP-choline:1,2-diacylglycerol choline phosphotransferase are membrane-bound enzymes with a substrate selectivity that is limited to *sn*-1,2 DAG. Both the "wrong" stereochemical structure of lipolysis-derived DAGs and their "mislocalization" on LDs makes it unlikely that they are endogenous substrates for DAG kinases or CDP-choline:1,2-diacylglycerol choline phosphotransferase without prior transesterification and translocation.

To investigate whether lipolysis-derived DAGs can serve as substrates for DGAT-mediated TAG formation, we analyzed the stereo/regioselectivity for this reaction. To date, the stereo/regioselectivity of DGAT1 and -2 is unknown. Our results clearly demonstrate that both DGAT1 and DGAT2 can esterify the ATGL products *sn*-1,3 and *sn*-2,3 DAG, although with different efficiencies. Whereas DGAT1 converts *rac*-1,2/2,3 more efficiently than *sn*-1,3 DAG, DGAT2 exhibits the opposite substrate selectivity. The different substrate specificities of DGAT1 and -2 may be explained by their structural differences. DGAT1 and -2 share no amino acid sequence homology and belong to unrelated protein families. DGAT1 belongs to the family of membrane-bound *O*-acyltransferases (MBOAT), but DGAT2 does not (46). Because of these structural differences, DGAT1 and -2 are also unable to functionally compensate for each other, as is evident from the very different phenotypes of the respective knock-out mouse lines (19, 47). Whereas DGAT1ko mice exhibit a relatively mild phenotype characterized by a reduction in TAG content in various tissues (47), DGAT2ko mice die shortly after birth due to a severe defect in skin barrier function (19). Both DGATs localize to the ER. Additionally, DGAT2 also associates with cytosolic LDs (22, 48). The findings that DGAT2 is present on LDs and prefers *sn*-1,3 DAGs as its acyl acceptor suggest that this enzyme may re-esterify DAG to TAG during basal lipolysis. It is estimated that at least one-third of lipolytic DAGs are re-esterified to TAG within a futile cycle (49).

In summary, our observations together with previously published data support a "three-pool" model for cellular DAGs (Fig. 9). Pool 1 consists of *sn*-1,2 DAG, which is generated during *de novo* lipogenesis in the ER. This pool is metabolized by DGAT enzymes and CDP-choline:1,2-diacylglycerol choline phosphotransferase. Pool 2 comprises *sn*-1,3 DAG ± *sn*-2,3 DAG generated by ATGL ± CGI-58 on LDs. TAG-derived DAGs are accessible to HSL-mediated catabolism or DGAT2-mediated TAG synthesis. Pool 3 (*sn*-1,2 DAG) is generated by PLCs on the plasma and ER membrane and can again serve as a precursor of phospholipid synthesis via phosphorylation catalyzed by DAG kinase or is degraded by membrane-bound DAG lipases. Additionally, this DAG pool can activate PKCs. The local separation as well as the stereo/regiochemical differences between DAG pools may provide an explanation to previously confusing data concerning DAG signaling and metabolism (50).

REFERENCES

1. Suzuki, M., Shinohara, Y., Ohsaki, Y., and Fujimoto, T. (2011) Lipid droplets. Size matters. *J. Electron. Microsc.* **60,** Suppl. 1, S101–S116
2. Osuga, J., Ishibashi, S., Oka, T., Yagyu, H., Tozawa, R., Fujimoto, A., Shionoiri, F., Yahagi, N., Kraemer, F. B., Tsutsumi, O., and Yamada, N. (2000) Targeted disruption of hormone-sensitive lipase results in male sterility and adipocyte hypertrophy but not in obesity. *Proc. Natl. Acad. Sci. U.S.A.* **97,** 787–792
3. Haemmerle, G., Zimmermann, R., Hayn, M., Theussl, C., Waeg, G., Wagner, E., Sattler, W., Magin, T. M., Wagner, E. F., and Zechner, R. (2002) Hormone-sensitive lipase deficiency in mice causes diglyceride accumulation in adipose tissue, muscle, and testis. *J. Biol. Chem.* **277,** 4806–4815
4. Haemmerle, G., Lass, A., Zimmermann, R., Gorkiewicz, G., Meyer, C., Rozman, J., Heldmaier, G., Maier, R., Theussl, C., Eder, S., Kratky, D., Wagner, E. F., Klingenspor, M., Hoefler, G., and Zechner, R. (2006) Defective lipolysis and altered energy metabolism in mice lacking adipose triglyceride lipase. *Science* **312,** 734–737
5. Taschler, U., Radner, F. P., Heier, C., Schreiber, R., Schweiger, M., Schoiswohl, G., Preiss-Landl, K., Jaeger, D., Reiter, B., Koefeler, H. C., Wojciechowski, J., Theussl, C., Penninger, J. M., Lass, A., Haemmerle, G.,

Zechner, R., and Zimmermann, R. (2011) Monoglyceride lipase deficiency in mice impairs lipolysis and attenuates diet-induced insulin resistance. *J. Biol. Chem.* **286,** 17467–17477
6. Lefèvre, C., Jobard, F., Caux, F., Bouadjar, B., Karaduman, A., Heilig, R., Lakhdar, H., Wollenberg, A., Verret, J. L., Weissenbach, J., Ozgüc, M., Lathrop, M., Prud'homme, J. F., and Fischer, J. (2001) Mutations in CGI-58, the gene encoding a new protein of the esterase/lipase/thioesterase subfamily, in Chanarin-Dorfman syndrome. *Am. J. Hum. Genet.* **69,** 1002–1012
7. Fischer, J., Lefèvre, C., Morava, E., Mussini, J. M., Laforêt, P., Negre-Salvayre, A., Lathrop, M., and Salvayre, R. (2007) The gene encoding adipose triglyceride lipase (PNPLA2) is mutated in neutral lipid storage disease with myopathy. *Nat. Genet.* **39,** 28–30
8. Zimmermann, R., Strauss, J. G., Haemmerle, G., Schoiswohl, G., Birner-Gruenberger, R., Riederer, M., Lass, A., Neuberger, G., Eisenhaber, F., Hermetter, A., and Zechner, R. (2004) Fat mobilization in adipose tissue is promoted by adipose triglyceride lipase. *Science* **306,** 1383–1386
9. Fredrikson, G., Strålfors, P., Nilsson, N. O., and Belfrage, P. (1981) Hormone-sensitive lipase of rat adipose tissue. Purification and some properties. *J. Biol. Chem.* **256,** 6311–6320
10. Tornqvist, H., and Belfrage, P. (1976) Purification and some properties of a monoacylglycerol-hydrolyzing enzyme of rat adipose tissue. *J. Biol. Chem.* **251,** 813–819
11. Lass, A., Zimmermann, R., Haemmerle, G., Riederer, M., Schoiswohl, G., Schweiger, M., Kienesberger, P., Strauss, J. G., Gorkiewicz, G., and Zechner, R. (2006) Adipose triglyceride lipase-mediated lipolysis of cellular fat stores is activated by CGI-58 and defective in Chanarin-Dorfman Syndrome. *Cell Metab.* **3,** 309–319
12. Granneman, J. G., Moore, H. P., Krishnamoorthy, R., and Rathod, M. (2009) Perilipin controls lipolysis by regulating the interactions of AB-hydrolase containing 5 (Abhd5) and adipose triglyceride lipase (Atgl). *J. Biol. Chem.* **284,** 34538–34544
13. Zechner, R., Zimmermann, R., Eichmann, T. O., Kohlwein, S. D., Haemmerle, G., Lass, A., and Madeo, F. (2012) Fat Signals. Lipases and lipolysis in lipid metabolism and signaling. *Cell Metab.* **15,** 279–291
14. Rogalska, E., Cudrey, C., Ferrato, F., and Verger, R. (1993) Stereoselective hydrolysis of triglycerides by animal and microbial lipases. *Chirality* **5,** 24–30
15. Boni, L. T., and Rando, R. R. (1985) The nature of protein kinase C activation by physically defined phospholipid vesicles and diacylglycerols. *J. Biol. Chem.* **260,** 10819–10825
16. Rando, R. R., and Young, N. (1984) The stereospecific activation of protein kinase C. *Biochem. Biophys. Res. Commun.* **122,** 818–823
17. Nomura, H., Ase, K., Sekiguchi, K., Kikkawa, U., Nishizuka, Y., Nakano, Y., and Satoh, T. (1986) Stereospecificity of diacylglycerol for stimulus-response coupling in platelets. *Biochem. Biophys. Res. Commun.* **140,** 1143–1151
18. Schweiger, M., Schoiswohl, G., Lass, A., Radner, F. P., Haemmerle, G., Malli, R., Graier, W., Cornaciu, I., Oberer, M., Salvayre, R., Fischer, J., Zechner, R., and Zimmermann, R. (2008) The C-terminal region of human adipose triglyceride lipase affects enzyme activity and lipid droplet binding. *J. Biol. Chem.* **283,** 17211–17220
19. Stone, S. J., Myers, H. M., Watkins, S. M., Brown, B. E., Feingold, K. R., Elias, P. M., and Farese, R. V., Jr. (2004) Lipopenia and skin barrier abnormalities in DGAT2-deficient mice. *J. Biol. Chem.* **279,** 11767–11776
20. Sattler, W., Puhl, H., Hayn, M., Kostner, G. M., and Esterbauer, H. (1991) Determination of fatty acids in the main lipoprotein classes by capillary gas chromatography. BF3/methanol transesterification of lyophilized samples instead of Folch extraction gives higher yields. *Anal. Biochem.* **198,** 184–190
21. Folch, J., Lees, M., and Sloane Stanley, G. H. (1957) A simple method for the isolation and purification of total lipides from animal tissues. *J. Biol. Chem.* **226,** 497–509
22. Stone, S. J., Levin, M. C., Zhou, P., Han, J., Walther, T. C., and Farese, R. V., Jr (2009) The endoplasmic reticulum enzyme DGAT2 is found in mitochondria-associated membranes and has a mitochondrial targeting signal that promotes its association with mitochondria. *J. Biol. Chem.* **284,** 5352–5361
23. Itabashi, Y., Kukis, A., Marai, L., and Takagi, T. (1990) HPLC resolution of diacylglycerol moieties of natural triacylglycerols on a chiral phase consisting of bonded (*R*)-(+)-1-(1-naphthyl)ethylamine. *J. Lipid Res.* **31,** 1711–1717
24. Jenkins, C. M., Mancuso, D. J., Yan, W., Sims, H. F., Gibson, B., and Gross, R. W. (2004) Identification, cloning, expression, and purification of three novel human calcium-independent phospholipase A2 family members possessing triacylglycerol lipase and acylglycerol transacylase activities. *J. Biol. Chem.* **279,** 48968–48975
25. Turban, S., and Hajduch, E. (2011) Protein kinase C isoforms. Mediators of reactive lipid metabolites in the development of insulin resistance. *FEBS Lett.* **585,** 269–274
26. Ahn, K., McKinney, M. K., and Cravatt, B. F. (2008) Enzymatic pathways that regulate endocannabinoid signaling in the nervous system. *Chem. Rev.* **108,** 1687–1707
27. Gibellini, F., and Smith, T. K. (2010) The Kennedy pathway. *De novo* synthesis of phosphatidylethanolamine and phosphatidylcholine. *IUBMB Life* **62,** 414–428
28. van Tienhoven, M., Atkins, J., Li, Y., and Glynn, P. (2002) Human neuropathy target esterase catalyzes hydrolysis of membrane lipids. *J. Biol. Chem.* **277,** 20942–20948
29. Kienesberger, P. C., Lass, A., Preiss-Landl, K., Wolinski, H., Kohlwein, S. D., Zimmermann, R., and Zechner, R. (2008) Identification of an insulin-regulated lysophospholipase with homology to neuropathy target esterase. *J. Biol. Chem.* **283,** 5908–5917
30. Yan, W., Jenkins, C. M., Han, X., Mancuso, D. J., Sims, H. F., Yang, K., and Gross, R. W. (2005) The highly selective production of 2-arachidonoyl lysophosphatidylcholine catalyzed by purified calcium-independent phospholipase A2γ. Identification of a novel enzymatic mediator for the generation of a key branch point intermediate in eicosanoid signaling. *J. Biol. Chem.* **280,** 26669–26679
31. Tang, J., Kriz, R. W., Wolfman, N., Shaffer, M., Seehra, J., and Jones, S. S. (1997) A novel cytosolic calcium-independent phospholipase A2 contains eight ankyrin motifs. *J. Biol. Chem.* **272,** 8567–8575
32. Carrière, F., Rogalska, E., Cudrey, C., Ferrato, F., Laugier, R., and Verger, R. (1997) *In vivo* and *in vitro* studies on the stereoselective hydrolysis of tri- and diglycerides by gastric and pancreatic lipases. *Bioorg. Med. Chem.* **5,** 429–435
33. Paltauf, F., Esfandi, F., and Holasek, A. (1974) Stereospecificity of lipases. Enzymic hydrolysis of enantiomeric alkyl diacylglycerols by lipoprotein lipase, lingual lipase, and pancreatic lipase. *FEBS Lett.* **40,** 119–123
34. Jensen, R. G., DeJong, F. A., Clark, R. M., Palmgren, L. G., Liao, T. H., and Hamosh, M. (1982) Stereospecificity of premature human infant lingual lipase. *Lipids* **17,** 570–572
35. Rogalska, E., Ransac, S., and Verger, R. (1993) Controlling lipase stereoselectivity via the surface pressure. *J. Biol. Chem.* **268,** 792–794
36. Morley, N., and Kuksis, A. (1972) Positional specificity of lipoprotein lipase. *J. Biol. Chem.* **247,** 6389–6393
37. Wang, C. S., Kuksis, A., Manganaro, F., Myher, J. J., Downs, D., and Bass, H. B. (1983) Studies on the substrate specificity of purified human milk bile salt-activated lipase. *J. Biol. Chem.* **258,** 9197–9202
38. Rodriguez, J. A., Ben Ali, Y., Abdelkafi, S., Mendoza, L. D., Leclaire, J., Fotiadu, F., Buono, G., Carrière, F., and Abousalham, A. (2010) *In vitro* stereoselective hydrolysis of diacylglycerols by hormone-sensitive lipase. *Biochim. Biophys. Acta* **1801,** 77–83
39. Samuel, V. T., Petersen, K. F., and Shulman, G. I. (2010) Lipid-induced insulin resistance. Unraveling the mechanism. *Lancet* **375,** 2267–2277
40. Erion, D. M., and Shulman, G. I. (2010) Diacylglycerol-mediated insulin resistance. *Nat. Med.* **16,** 400–402
41. Voshol, P. J., Haemmerle, G., Ouwens, D. M., Zimmermann, R., Zechner, R., Teusink, B., Maassen, J. A., Havekes, L. M., and Romijn, J. A. (2003) Increased hepatic insulin sensitivity together with decreased hepatic triglyceride stores in hormone-sensitive lipase-deficient mice. *Endocrinology* **144,** 3456–3462
42. Harada, K., Shen, W. J., Patel, S., Natu, V., Wang, J., Osuga, J., Ishibashi, S., and Kraemer, F. B. (2003) Resistance to high-fat diet-induced obesity and altered expression of adipose-specific genes in HSL-deficient mice. *Am. J. Physiol. Endocrinol. Metab.* **285,** E1182–E1195

43. Park, S. Y., Kim, H. J., Wang, S., Higashimori, T., Dong, J., Kim, Y. J., Cline, G., Li, H., Prentki, M., Shulman, G. I., Mitchell, G. A., and Kim, J. K. (2005) Hormone-sensitive lipase knockout mice have increased hepatic insulin sensitivity and are protected from short-term diet-induced insulin resistance in skeletal muscle and heart. *Am. J. Physiol. Endocrinol. Metab.* **289,** E30–E39
44. Mulder, H., Sörhede-Winzell, M., Contreras, J. A., Fex, M., Ström, K., Ploug, T., Galbo, H., Arner, P., Lundberg, C., Sundler, F., Ahrén, B., and Holm, C. (2003) Hormone-sensitive lipase null mice exhibit signs of impaired insulin sensitivity, whereas insulin secretion is intact. *J. Biol. Chem.* **278,** 36380–36388
45. Roduit, R., Masiello, P., Wang, S. P., Li, H., Mitchell, G. A., and Prentki, M. (2001) A role for hormone-sensitive lipase in glucose-stimulated insulin secretion. A study in hormone-sensitive lipase-deficient mice. *Diabetes* **50,** 1970–1975
46. Yen, C. L., Stone, S. J., Koliwad, S., Harris, C., and Farese, R. V., Jr (2008) Thematic review series. Glycerolipids. DGAT enzymes and triacylglycerol biosynthesis. *J. Lipid Res.* **49,** 2283–2301
47. Chen, H. C., Smith, S. J., Ladha, Z., Jensen, D. R., Ferreira, L. D., Pulawa, L. K., McGuire, J. G., Pitas, R. E., Eckel, R. H., and Farese, R. V., Jr (2002) Increased insulin and leptin sensitivity in mice lacking acyl CoA:diacylglycerol acyltransferase 1. *J. Clin. Invest.* **109,** 1049–1055
48. McFie, P. J., Banman, S. L., Kary, S., and Stone, S. J. (2011) Murine diacylglycerol acyltransferase-2 (DGAT2) can catalyze triacylglycerol synthesis and promote lipid droplet formation independent of its localization to the endoplasmic reticulum. *J. Biol. Chem.* **286,** 28235–28246
49. Reshef, L., Olswang, Y., Cassuto, H., Blum, B., Croniger, C. M., Kalhan, S. C., Tilghman, S. M., and Hanson, R. W. (2003) Glyceroneogenesis and the triglyceride/fatty acid cycle. *J. Biol. Chem.* **278,** 30413–30416
50. Farese, R. V., Jr, Zechner, R., Newgard, C. B., and Walther, T. C. (2012) The problem of establishing relationships between hepatic steatosis and hepatic insulin resistance. *Cell Metab.* **15,** 570–573